DEEP-HEAT-FLOWS: DISCOVERING DEEP GEOTHERMAL RESOURCES IN LOW-ENTHALPY CRYSTALLINE SETTINGS

Progress Report, 21.10.2024

1- Project Progress:

All tasks and actions are on track or have been completed ahead of schedule (Figure 1).

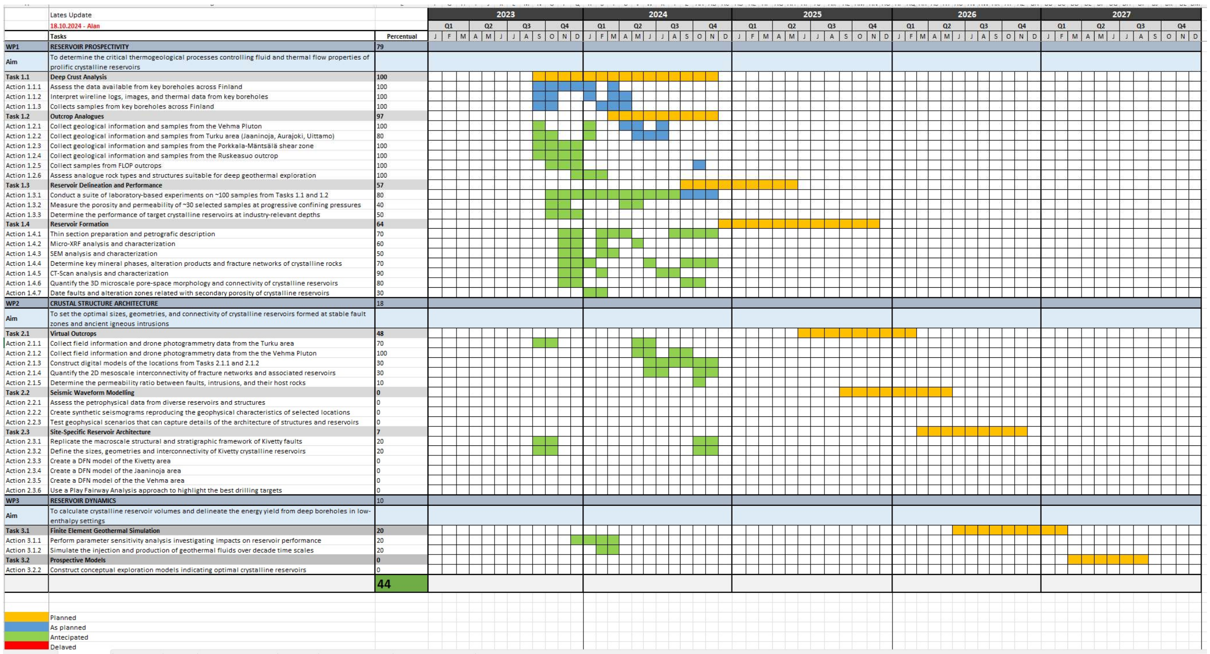

Boreholes analysed	Outcrops described	Standard petrophysics	Detailed Vp-Vs	Porosity confining pressure	Permeability confining pressure	Permeability unconfining pressure
62	8	327	120	1	11	46
Thin-sections	**CT scan**	**Micro-XRF**	**EDS-SEM**	**Isotopes**	**Drone photogrammetry**	
86	29	21	6	7	8	
Standard petrophysics include: porosity, density, P-wave velocity, magnetic susceptibility, resistivity, thermal conductivity, and heat capacity.						

Figure 1: Gantt chart of the project summarizing the actions and tasks forecasted for the project, along with performance indicators for achievements.

Task 1.1 Deep Crust Analysis is nearly complete. We have assessed well data from fifteen locations across Finland (Figure 2). From these, seven locations have been selected for further study, including:

- Koillismaa: 2 wells up to 1,724 m deep
- Kivetty: 13 wells up to 1,000 m deep
- Mäntsälä: 2 wells up to 1,000 m deep
- Loviisa: 9 wells up to 1,000 m deep
- Otaniemi: 3 wells up to 6,400 m deep
- Vantaa: 27 wells up to 200 m deep
- Kopparnäs: 16 wells up to 230 m deep

Sample collection from Loviisa is scheduled for December 2024, and data interpretation from all locations is still ongoing.

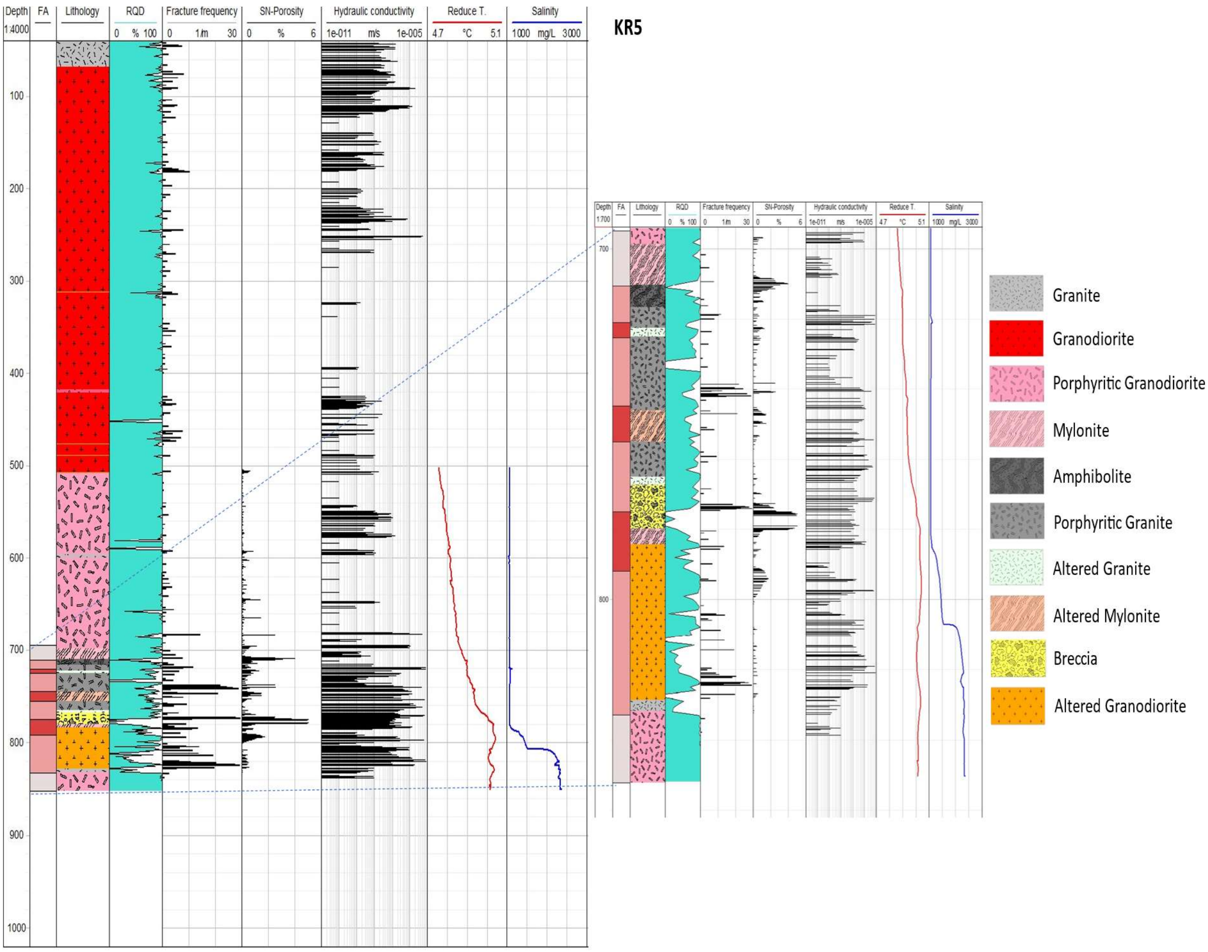

Figure 2: Example of a composite well data from the Kivetty area.

Eight areas were selected for **outcrop analogue studies (Task 1.2)**, including Turku (Jaaninoja, Aurajoki, Uittamo fault systems), Kasavuori, Ruskeasuo, Laajalahti, Vehmaa Batholith, Kopparnäs, Åland, and the Paimio Shear Zone. Baseline studies in Kasavuori, Ruskeasuo, Laajalahti, Kopparnäs, Åland, and Paimio are completed, while detailed studies are ongoing in the Turku and Vehmaa areas.

Reservoir Delineation and Performance (Task 1.4) is well advanced. We have collected 768 samples, of which 327 were sent for standard petrophysical analysis (Figure 3). The results for most of these samples are now available, including measurements of porosity, density, P-wave velocity, magnetic susceptibility, resistivity, thermal conductivity, and heat capacity. Permeability at unconfined pressure was measured from 46 of these samples, while permeability at up to 50 MPa confining pressure was measured from 11 samples, and porosity at up to 50 MPa confining pressure was measured from only 1 sample. Detailed Vp-Vs seismic wave velocity measurements are underway at the Rock Physics Finland laboratory and will be the focus of Wassem Ullah's MSc thesis. Further porosity and permeability tests at confining pressure are scheduled for February 2025 at the University of Strasbourg, France, guided by Michael Heap. Radiogenic heat production analysis is planned to be conducted at the University of Turku, with work scheduled to begin in late winter 2025. Geomechanical tests are under discussion with Roberto Rizzo from Utrecht University.

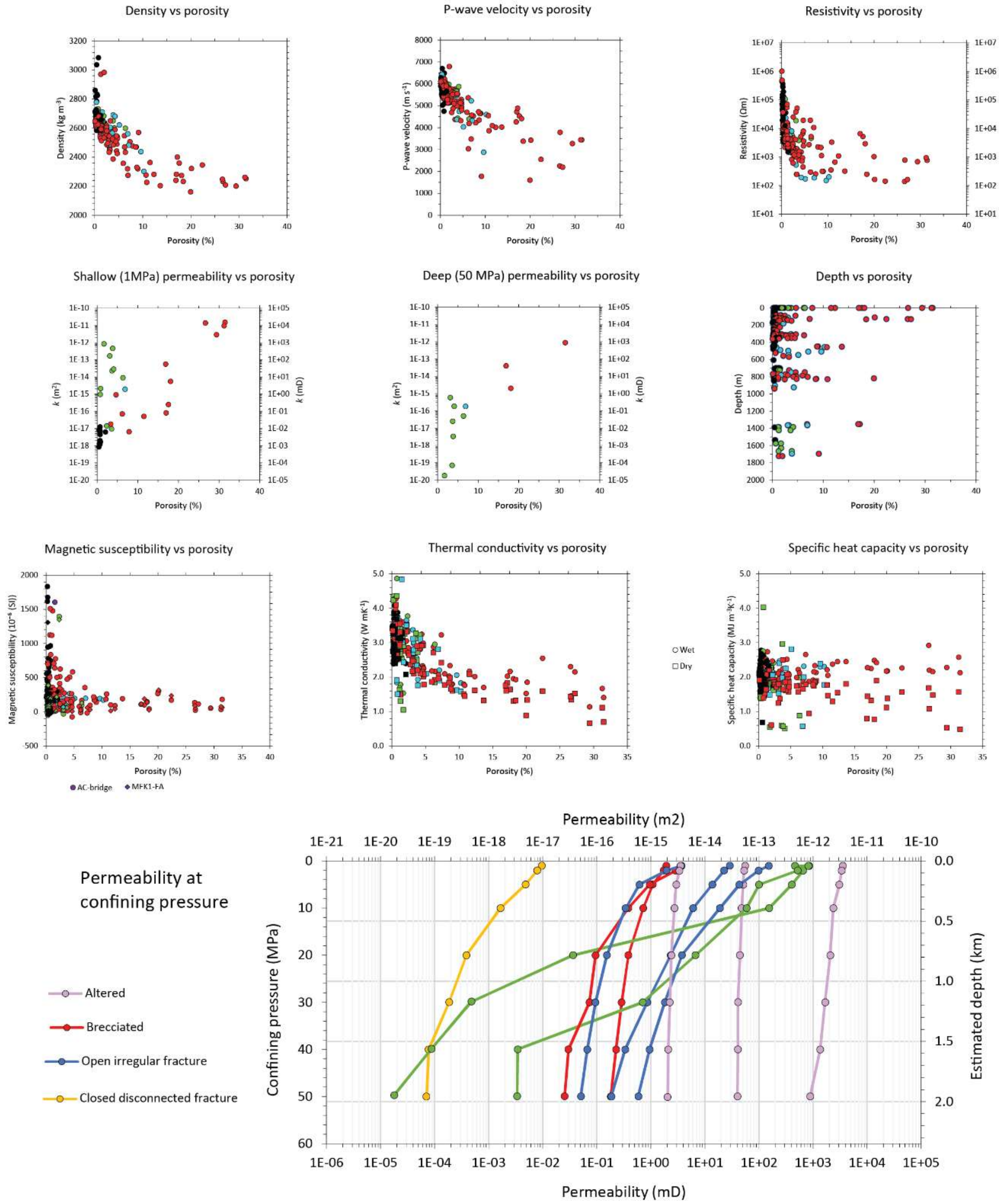

Figure 3: Main petrophysics trends observed on Finnish crystalline rocks, sorted by their texture and structure. Black dot = massive; green = fracture; blue = brecciated; red = altered.

Reservoir Formation (Task 1.4) studies are progressing rapidly. We have prepared, described, and photographed 86 thin sections of target rock facies (Figure 4), completed 29 3D CT-scan tomography images (Figure 5), performed 21 Micro-XRF analyses, and analyzed 6 samples for SEM-EDS. Additionally, we dated 1 fault using the Illite K-Ar method and 6 samples containing secondary titanite using the U-Pb method. Rock-fluid reaction experiments are underway with EPFL, Switzerland, led by Alexandra Kushnir.

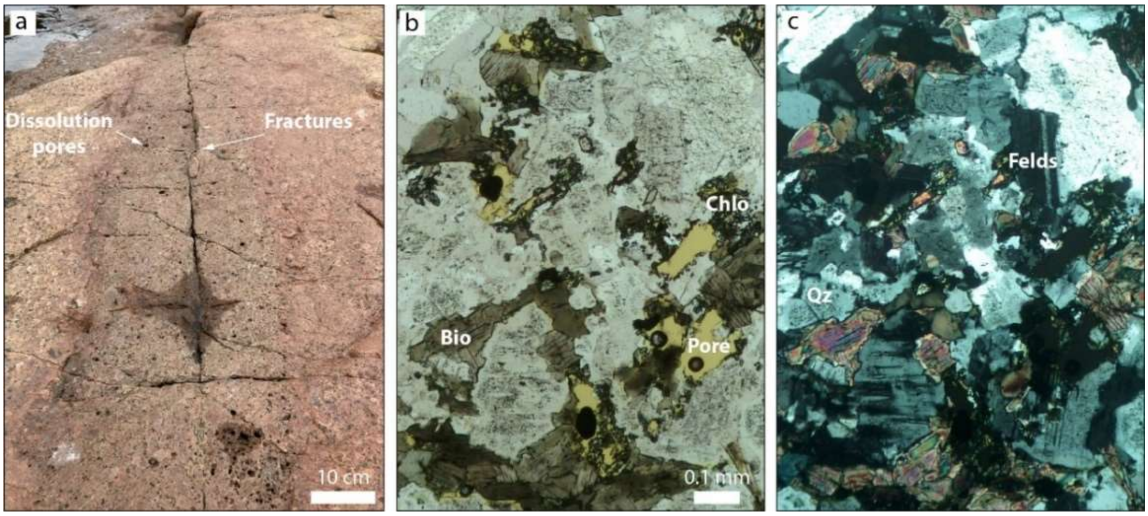

Figure 4: Examples of crystalline rocks affected by fracturing and hydrothermal alteration. (a) Rapakivi granite from the Vehmaa Batholith, Southern Finland. Microphotographs in natural (b) and plain polarized light (c) of an altered granite collected from a depth of 1620 m from the Koillismaa borehole, Eastern Finland.

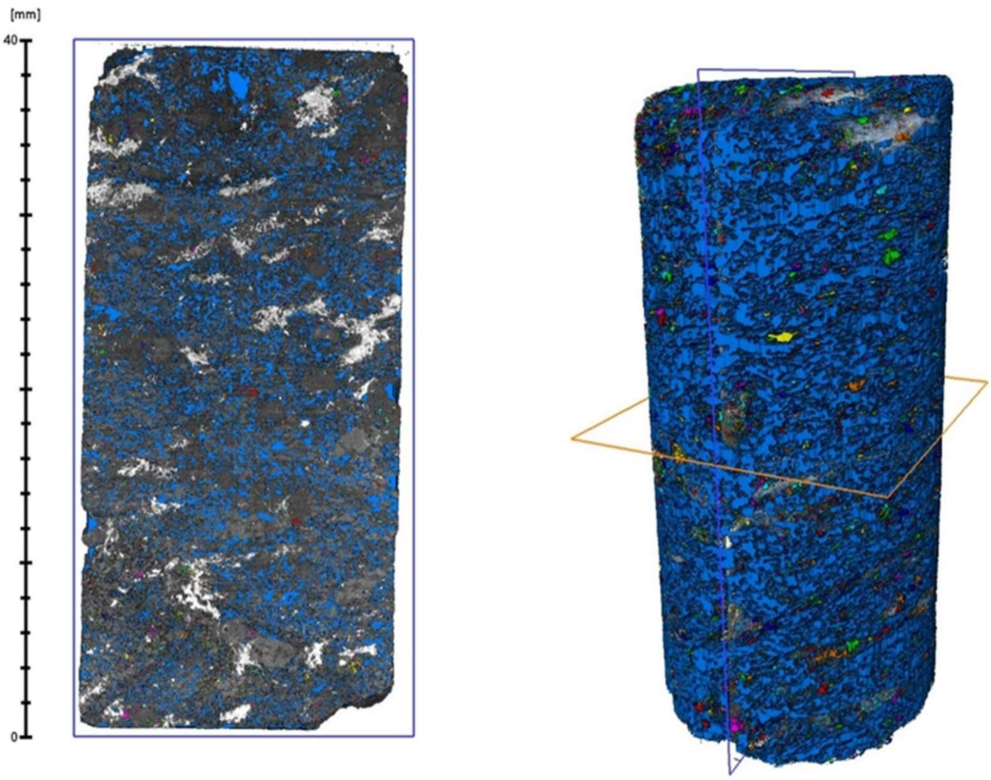

Figure 5: An example of 3D tomography of a drill core from the Kivetty area. Blue color corresponds to the connected porosity of the rock.

The construction of **virtual outcrops (Task 2.1)** is ahead of schedule (Figure 6). We have collected drone images from 2 areas in Turku and 6 locations in the Vehmaa Batholith. Fault and fracture interpretation is complete in the Vehmaa Batholith and is the subject of Pelayo Barron's PhD thesis in the Turku area, which will be complemented by further drone acquisitions scheduled for completion in 2024.

Task 2.2, Seismic Waveform Modelling, hasn't started yet, while **Task 2.3, Site-Specific Reservoir Architecture**, is underway in the Kivetty area (Figure 7). **Finite element geothermal simulations (task 3.1)** were performed for three hypothetical reservoirs and will continue as the project evolves (Figure 8).

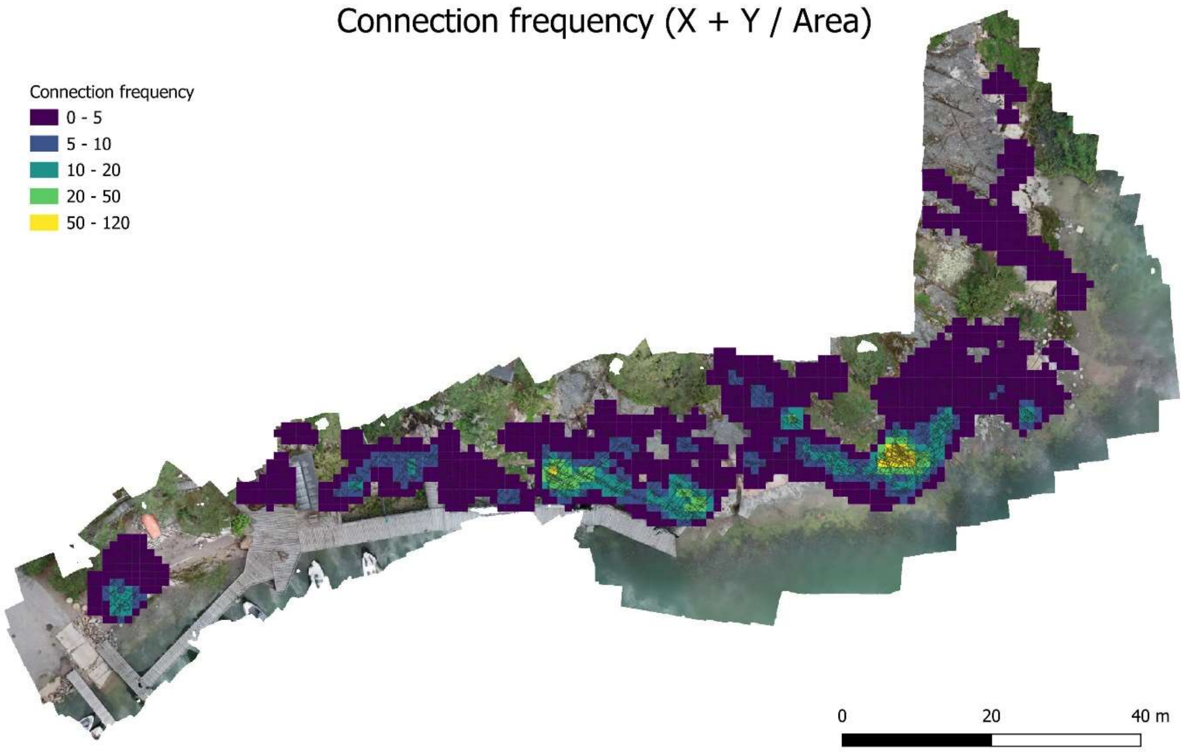

Figure 6: Topology interpretation from an area in the Vehmaa Batholith.

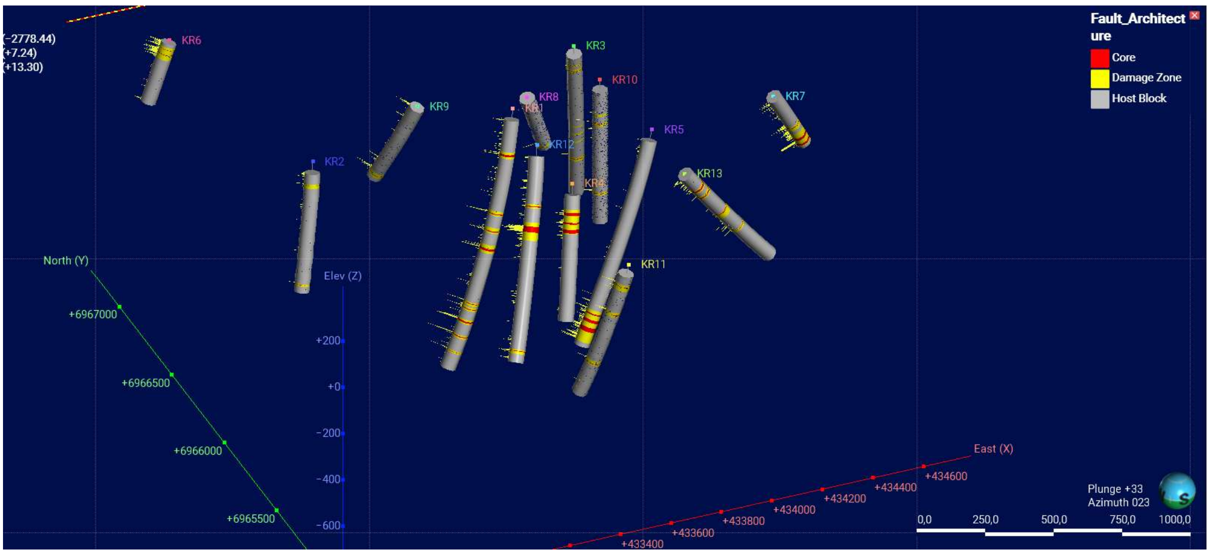

Figure 7: An initial geological-structural modelling at the Kivetty site.

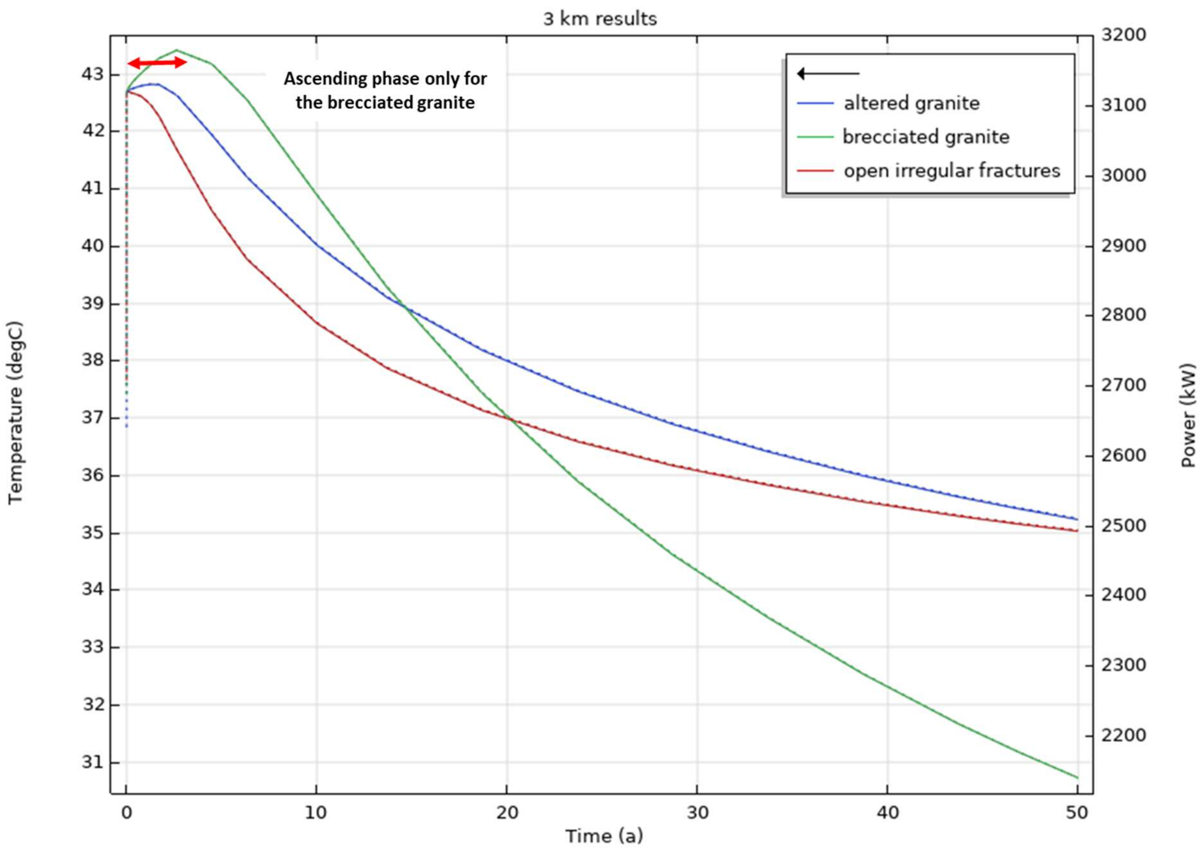

Figure 8: Hypothetical simulation of geothermal reservoir production.

2- Preliminary findings

Petrophysical parameters of crystalline reservoirs

Our preliminary findings highlight a consistent trend among various petrophysical parameters: rock density, electric resistivity, elastic wave velocity, magnetic susceptibility, thermal conductivity, and heat capacity typically decrease as porosity increases, a pattern classically observed across sedimentary and volcanic rocks. Additionally, porosity and permeability are usually directly proportional and governed by the extent of brittle deformation and alteration processes affecting the crystalline rocks. Thus, altered rocks have the higher porosity and permeability values, up to 31.5% and 1.5×10^{-11} m^2 (15.2 Darcy), respectively; brecciated and fractured rocks have moderate porosity ranging from 1 to 10% and permeability up to 8.38×10^{-13} m^2 (849 millidarcy); while massive rocks recorded the lowest porosity (<2%) and permeability ($<1.23 \times 10^{-17}$ m^2) values. Markedly, these rocks are consistently distributed across diverse parts of fault zones. Typically, altered, brecciated, and fractured rocks are found in the fault core and damage zone, while massive rocks occur within the host block. However, massive rocks can also occur in the damage zone and fault core. Notably, all rocks with porosity above 10% are highly altered and consistently located within the fault core, a zone characterized by intense deformation where most of the fault displacement occurs. This observation highlights that porosity (and consequently other properties such permeability, density, resistivity, elastic wave velocity, and thermal parameters) systematically varies following the fault architecture, providing a valuable prospective model for locating geothermal reservoirs in crystalline settings. In detail, the quality of crystalline reservoir (i.e. their suitability for geothermal energy extraction) is primarily revealed by the morphology and connectivity of diverse pore types. Massive rocks typically have dispersed and disconnected pores and thus have little reservoir potential. Their value in geothermal systems relies on their ability to store and transfer heat by conduction, due to abundant minerals such as quartz and feldspar, as well as to generate heat through the decay of radioactive elements like uranium, thorium, and potassium. Conversely, rocks dominated by fractures typically have low porosity (<5%) but can exhibit extremely high permeability (nearly 10^{-12} m^2) at low confining pressure, which sharply decreases to 10^{-19} m^2 when confining pressure exceeds 20–30 MPa, corresponding to depths of around 700–1000 meters. According to our dataset, only fractures with irregular walls commonly resulting from mineral dissolution and brecciation can sustain permeability above 10^{-16} m^2 at high confining pressures of 50 MPa, simulating depths of approximately 2 km. Consequently, rocks that have undergone brecciation and hydrothermal alteration are the most promising deep geothermal reservoirs because they show comparatively milder porosity and permeability reduction even under high confining pressures of 50 MPa.

Crystalline reservoir formation in Fennoscandia

Throughout most subsets of rocks transected by faults and fractures, a consistent pattern emerge: mafic minerals including biotite, pyroxene and amphibole are commonly replaced by chlorite and epidote, indicating hydrothermal alteration processes at relatively high temperatures (200–300 °C). Additionally, altered peraluminous granites, migmatites and gneisses display a replacement order of garnet→biotite→chlorite→titanite, which is consistent with retrograde metamorphism and hydration also at relatively high temperature. We observe that the effects of hydrothermal alteration and leaching of mafic mineral phases, plagioclase, and garnet are often associated with the generation of secondary porosity. This includes the development of moldic, intracrystal, and sieve pores, typically achieving 60% and up to 96% pore connectivity at an 11 µm CT scan resolution. As thermal and tectonic events of great magnitude have not been reported to substantially affect the Fennoscandian upper crust in the last billion years, most faulting and hydrothermal alteration must date from Precambrian times. We perform U-Pb isotope dating of secondary titanite to serve as a proxy for the age of porosity formation at a location in the Karelian Craton. The age results cluster at 2200-2140 Ma and 1900-1750 Ma, confirming a temporal correlation with the Paleoproterozoic rifting of the Karelian Craton and the Svecofennian orogeny. Although the relationship between hydrothermal alteration and secondary porosity exerts a first-order control throughout our dataset, the overprinting effects of weathering due to the exposure of the crystalline rocks to meteoric water and organic fluids is also commonly observed, particularly in rock samples collected from outcrops or from shallow (<500 m) borehole sections. In light of our observations, we describe the formation of crystalline reservoirs as a dynamic process that likely involves multiple interrelated tectonic, thermal, and chemical stages: Initially, massive rocks were fractured and brecciated by tectonic forces or hydro-mechanical stress, creating pathways for fluid circulation. Hydrothermal fluids then use these fracture pathways and interact with primary minerals, inducing chemical alterations and leaching, which lead to the generation of secondary porosity. When finally exposed to meteoric and organic fluids, the porosity initially created at higher temperature conditions is further reshaped by additional mineral dissolution processes and the precipitation of new mineral phases and oxides. These processes can be repeated multiple times as faults are reactivated under new stress regimes or during younger magmatic and orogenic events.

Permeability and Connectivity of Fault Zones

In the Kivetty area, our findings show that altered and fractured rocks significantly enhance fluid flow connectivity. We described several fractured and altered intervals with porosity of nearly 20%. Legacy cross-flow pumping tests indicate that these zones can extend laterally for at least 500 m. Hydrothermal alterations, dominated by the dissolution of feldspar, K-feldspar, quartz, and biotite, and the precipitation of chlorite, epidote, Fe-oxides, Ti-oxides, and muscovite, suggest formation under high temperatures (exceeding 200 °C), with overprinted lower-temperature meteoric alteration. These alterations increase porosity (up to 20%) and permeability (up to 10^{-12} m^2) in fault zones, with pore connectivity up to 94% as measured by CT scans at 11-micron resolution. In contrast, unaltered host rocks exhibit much lower porosity (~1%) and permeability (<10^{-17} m^2).

Characterization of brittle structures and reservoirs within the Vehmaa Batholith

Our 1:200 000 scale lineament analysis of the Vehmaa rapakivi granite revealed two main sets of lineaments with NNW and ENE trends, which contrast with the regional NNE orientation of major lineaments within the surrounding Paleoproterozoic bedrock. The NNW lineaments are relatively continuous over several kilometers, while the ENE lineaments typically terminate against the NNW lineaments, suggesting that the ENE lineaments are younger. In outcrop and drone photogrammetry, faults and fractured zones extend over tens to hundreds of meters and aligning consistently with the location and orientation of larger lineaments. The most prominent fault sets exhibit NW trends and strike-slip character. Furthermore, ENE trending strike-slip faults are also present, though they do not form a well-defined set but exhibit instead scattered E to NE trends. Paleostress analysis reveals two distinct stress regimes: one characterized by WNW–ESE compression and another by NNE–SSW compression, associated with transpressive and transtensive conditions, respectively. Our field and drone mapping revealed that many NW-trending strike-slip faults within the Vehmaa Batholith correlate with zones of pervasive mineral alteration. Typical mineral paragenesis within the alteration zones is chlorite, prehnite, and zeolite, indicating hydrothermal events of nearly 300 °C. Typically, the fractured and altered rocks within these zones display substantial porosity of ~10% and laboratory-measured permeabilities exceeding 2×10^{-15} m^2 under 50 MPa confining pressure. The strike-slip fault networks are hundreds-to-thousands of meters in total length and could form crystalline reservoirs with volumes exciding 1 km^3, which are promising targets for geothermal resources.

Geothermal production estimation

To provide a first-order estimation of heat production in a typical Finnish geothermal setting, we conducted a sensitivity analysis of hypothetical reservoirs based on our new petrophysical dataset. Results indicate that a 3 km-deep doublet Enhanced Geothermal System constructed within fault-related crystalline reservoirs could deliver an average power capacity of nearly 3 MWth over a 50-year production scenario.

3- Publications and other deliverables

We have published 1 peer-reviewed article, made 5 conference presentations, and delivered 4 scientific talks for stakeholders of the project. Publications can be downloaded from the Deep-HEAT-Flows website at https://deep-heat-flows.voog.com/publications